Title
Projectile Breakup of {sup 16}O at 32.5 Mev/A: Comparison of a Classical Dynamical Model with Experiment

Journal
Nuclear Physics A, 548

Authors
Suro, J.
Chan, Y.D.
Scarpaci, J.A.
et al.

Publication Date
1992-02-01

LBL-31957
Preprint

Lawrence Berkeley Laboratory
UNIVERSITY OF CALIFORNIA

Submitted to Nuclear Physics A

Projectile Breakup of ^{16}O at 32.5 MeV/A: Comparison of a Classical Dynamical Model with Experiment

J. Suro, Y.D. Chan, J.A. Scarpaci, R.G. Stokstad, K. Möhring, and T.C. Schmidt

February 1992

Prepared for the U.S. Department of Energy under Contract Number DE-AC03-76SF00098

DISCLAIMER

LBL-31957

Projectile Breakup of ^{16}O at 32.5 MeV/A: Comparison of a Classical Dynamical Model with Experiment

J. Suro, Y.D. Chan, J.A. Scarpaci, and R.G. Stokstad
Nuclear Science Division
Lawrence Berkeley Laboratory
University of California
Berkeley, CA 94720

and

K. Möhring and T.C. Schmidt
Bereich Schwerionenphysik, Hahn-Meitner-Institut Berlin,
Postfach 390128, D-1000 Berlin 39, Germany

February 1992

This work was supported by the Director, Office of Energy Research,
Office of High Energy and Nuclear Physics, Nuclear Physics Division of
the U.S. Department of Energy under Contract No. DE-AC03-76SF00098.

Projectile Breakup of ^{16}O at 32.5 MeV/A: Comparison of a Classical Dynamical Model with Experiment

J. Suro, Y.D. Chan, J.A. Scarpaci, and R.G. Stokstad

Nuclear Science Division, Lawrence Berkeley Laboratory,
Berkeley, CA 94720, USA

and

K. Möhring and T.C. Schmidt

Bereich Schwerionenphysik, Hahn-Meitner-Institut Berlin,
Postfach 390128, D-1000 Berlin 39, Germany

Abstract: A comparison is made of a classical dynamical model for the reaction of alpha-particle-conjugate projectiles on heavy targets with experimental data for the breakup of ^{16}O into four alpha particles. Theoretical events generated by a Monte Carlo method are "filtered" through the angular and energy constraints of the detector array. The agreement is good. The effects of the filtering and particle-particle correlations are discussed.

NUCLEAR REACTIONS $^{197}Au(^{16}O, 4\alpha)$, E=32.5 MeV/A; measured multiple breakup of projectile. Compared classical dynamical reaction model to experiment.

1. Introduction

Experiments that can detect all the fragments from the breakup of a projectile and theories that can predict the experimental observables should in principle enable us to distinguish between the extreme time scales of sequential decay and multifragmentation in a heavy-ion reaction. Only through comparisons of different models, employing different assumptions and physics, to the same experimental results can one hope to assess the reliability of the resulting conclusions.

The present study is an outgrowth of two recent comparisons of theory and experiment for light projectiles colliding with heavy targets. Harmon, et al., [1] compared the properties of the He+He+He+He channel produced [2] in the breakup of ^{16}O at 32.5 MeV/A by ^{197}Au with the kinematic signatures for sequential decay and multifragmentation predicted by Lopez and Randrup [3]. The reactions of ^{20}Ne with Au at 20 MeV/A have been studied in detail at the Hahn-Meitner Institute [4] and were compared recently [5] with the classical dynamical model of Möhring, et al. [5,6]. The former case emphasized the very peripheral breakup reactions while the latter focussed on reactions of the projectile leading to deep inelastic collisions. In both cases fairly good agreement between theory and experiment was obtained: the breakup of ^{16}O was consistent with a kinematical model for sequential decay (implying a long time scale) and offered no evidence for the multifragmentation of an isolated ^{16}O nucleus while the more damped interactions of Ne with Au were accounted for by a dynamical model in which the projectile dissociates promptly, i.e., while still in the field of the target.

Given the above observations, it is of interest to compare the classical dynamical model to the experimental data for the projectile breakup of ^{16}O because, in the model, peripheral and strongly damped collisions are treated on an equal footing and, second, the time scale for the dissociation of the projectile is prompt. In this comparison, therefore, we will test only a portion of the model, viz., those collisions with larger impact parameters that produce projectile fragments at sufficiently forward angles to be accepted by the detector array.

2. The model and its comparison to experiment

The classical dynamical model developed by Möhring and collaborators is described briefly in ref. 5 and in detail in ref. 6. In brief, the projectile is represented as a cluster of N alpha particles, which interact with each other via an α-α potential and with the target via an α-nucleus potential. The latter interaction is based on the conservative and frictional forces that have been used successfully in the description of dissipative or strongly damped heavy-ion collisions. The classical equations of motion for the N+1 body system are solved for a set of initial conditions chosen by a microcanonical Monte Carlo method. The alpha particles contained in the projectile may fuse with the target, interact with the target (as well as with each other) and appear as free alpha particles, or may be emitted as part of an alpha-particle cluster such as a ^{12}C or ^{8}Be nucleus. The velocities of all the reaction products are predicted, which enables a direct comparison with experiment. A total of about 200,000 collisions distributed uniformly over the impact parameter range from 5 fm to 11 fm (100 $\hbar$ to 220 $\hbar$) were generated.

The experimental apparatus is described in ref. 7 and consisted of an array of 34 phoswich detectors, centered about the beam axis in a 5x7 (horizontal x vertical) array. Each detector subtended approximately five degrees in the laboratory system. The threshold energy for identifying an alpha particle was about 9 MeV/A.

Our comparison of the classical dynamical model to the experimental data was made by examining the properties of each fragment in an event to determine if all of the fragments were in the angular and energy range covered by the detector array. Events passing through this filter were then analyzed in exactly the same manner as the events measured in the physical experiment. Distributions of both "filtered" and "unfiltered" theoretical events were examined in order to assess the effects of the angular coverage of the array on the comparison with the model.

The comparison focusses on the exit channel He+He+He+He because this channel contains the largest number of alpha particles and therefore offers the best opportunity to look for multiparticle correlations. In the following, we refer to the He nuclei detected in the experiment as alpha particles even though the detectors did not distinguish between ^{3}He and ^{4}He. Because of the negative Q-values associated with producing ^{3}He, however, it is reasonable to treat all Z=2 fragments as ^{4}He nuclei.

3. Results

3.1 Cross sections

The 197,562 collisions, when weighted with impact parameter, corresponded to a total cross section of 3550 mb and were distributed over the possible exit channels in the following manner. Thirty-six percent of the collisions produced an excited target nucleus but left the ^{16}O projectile intact. Thirty-five percent resulted in the transfer of one or more alpha particles to the target. The remaining 29 percent of the collisions produced the four reaction channels listed in Table 1.

It is immediately apparent from Table 1 that the more peripheral reactions observed in the experiment represent only about five percent of the corresponding reactions generated in the model. This is because the model was developed to describe damped interactions, which produce fragments at relatively large laboratory angles whereas the experiment was optimized for more forward-angle, peripheral reactions. That the angular range of the detector array ($\theta < 18$ degrees) preferentially selected reactions at larger impact parameters is illustrated in Fig. 1. The impact parameter distribution of all 4 α events (unfiltered) and of those 4 α events selected by the detector (filtered) are shown there. The shift to larger impact parameter for the filtered events is marked.

3.2 Singles alpha-particle angular distributions

These large differences in the filtered and unfiltered cross sections for the 4α channel are also reflected in the singles alpha particle angular distributions shown in Fig. 2. Note that the experimental angular distributions are more forward peaked than the theoretical predictions. This difference in slope, the absence of detectors beyond 18 degrees, and the requirement that all four alpha particles be detected account for the large differences in Table 1 (288 filtered events versus 14429 unfiltered). The normalization of the different curves in this figure was made as follows: the total number of alpha particles counted in the angular region from 5 to 18 degrees for the model (filtered) and for the experiment were normalized to each other for events in 4 α coincidence channel. This established the normalization for each of the remaining curves. The filtered and unfiltered theoretical results in Fig. 2 show that filtering does not have a large effect on the shape of the singles angular distribution.

3.3 Folding angle distribution

The directional correlations among the fragments contain information on the mechanism by which the projectile becomes excited and then dissociates. This was shown in ref. 3 for the folding angle defined by the two heaviest fragments. In ref. 1 a folding angle distribution was defined for the 4 α channel in the decay of ^{16}O from the opening angles between all combinations of alpha particles taken pair-wise, in the rest frame of the projectile. This experimental distribution is shown in Fig. 3.b. For reference, the solid curve shows the angular distribution predicted by Lopez and Randrup for the multifragmentation (i.e., prompt decay) of an isolated ^{16}O nucleus into 4 α particles.

Figure 3 shows the corresponding angular distribution predicted by the classical dynamical model for all events, i.e., unfiltered by the experimental conditions (Fig. 3.a), and for the filtered events (Fig. 3.b). The two important features of this comparison are that the experimental filter has a profound effect on the shape of this angular distribution and that the filtered theory agrees very well with experiment.

3.4 Sphericity and coplanarity

A similar situation occurs when the correlations among the four coincident alpha particles are represented in terms of sphericity and coplanarity (see ref. 3 for the definition and physical motivation of these quantities). Here again, the exclusion of events by the filtering effect of the experimental apparatus has a large effect on the average sphericity and coplanarity. The size and direction of this effect can be seen by comparing Figures 4.c and 4.b. The experimental result, shown in Fig. 4.a, and the filtered theoretical prediction, Fig. 4.b, agree very well. The mean values are given in Table 2.

3.5 Excitation energy

The total relative kinetic energy of the four alpha particles, when summed with the separation energy for $^{16}O \rightarrow 4\ \alpha$, corresponds to a total excitation energy in the primary ^{16}O nucleus. (This excitation energy is a well defined quantity and can be used for comparing experiment and theory even if there are final state interactions between the emerging alpha particles and the target.) The large apparent excitation energies in the unfiltered theoretical spectrum (Fig. 5.a) correspond to events in which one or two alpha particles are deflected to very large angles by the attractive nuclear force of the target nucleus. These events indicating a very high excitation energy are eliminated when the experimental filter is applied because the alpha particles at large angles simply miss the detector array. The filtered spectrum of excitation shown in Fig. 5.b, is much closer to experiment although the agreement is not complete. The number of counts in the theoretical and experimental spectra in Fig. 5.b are in the ratio of the corresponding cross sections given in Table 1.

4. Discussion

4.1 Cross sections

A precise comparison of the theoretical and experimental cross sections is complicated by several factors. On the experimental side, the cross sections for the three channels ^{8}Be+^{8}Be, ^{8}Be+2α, and 4 α are effectively summed together by the detector array. The 10.5 mb listed in Table 1 represents the sum of these three channels (see ref. 2). On the theoretical side, the model does not include odd-Z ejectiles. This increases the cross sections predicted for the even-Z fragments by up to a factor of two. Further more, the bound clusters of ^{8}Be produced in the calculation would make a contribution to the 4 α yield if they were forced to decay.

We can make a crude estimate of the contributions that the channels in the model containing ^{8}Be would make to the filtered 4 α channel by including the efficiency of the array for detecting the alpha particles from the ^{8}Be. Thus, the contribution of the ^{8}Be+^{8}Be channel is obtained by taking the ^{8}Be filtered cross section of 15 mb in Table 1 and multiplying it by the efficiency of the array (as described in ref. 2) for detecting four alpha particles (41%). Similarly, the filtered cross section for ^{8}Be+2α would be multiplied by 64%, the efficiency for detecting the two alpha particles from the single ^{8}Be. Adding these contributions to the 5.5 mb for the 4 α channel and dividing the total by two (to correct for the even-Z enhancement) yields 15 mb. Given the rough approximations in making this estimate, the value of 15 mb compares favorably with the experimental value of 10.5 $\pm$ 2 mb.

4.2 Singles alpha-particle angular distributions

The theoretical angular distributions for individual alpha particles shown in Fig. 2 do not agree with experiment over the angular range covered by the detector, the theoretical differential cross sections decreasing less rapidly with larger angles. The agreement with experiment would be improved by including explicitly in the calculation a post-collision decay of those long-lived clusters having a classical internal excitation energy in excess of a particle decay threshold [6]. (Long-lived clusters are ones that do not decay within the finite period of time for which the evolution of the cluster is followed in the dynamical calculation.) Such events represent the classical equivalent of inelastic excitation of the projectile followed by sequential decay, i.e, the excitation and decay of quantum states of the projectile. It is well known from many two-particle coincidence experiments that this is a strong mechanism, and that it is forward-peaked [8-10].

4.3 Directional correlations

The agreement of the classical dynamical model with experiment in the case of the folding angle distribution (Fig. 3.b) is indeed remarkable. In ref. 1 it was shown that the experimental folding angle distribution and the prediction for sequential decay were essentially identical. In the sequential case the only constraints on the emission energies and angles of the alpha particles are conservation of energy and momentum. In the present case we see that the classical dynamical model - in which the trajectory of each alpha particle is calculated according to the dynamics of that collision - gives an identical result *for the subset of events accepted by the detector.* There are two factors that must be considered in assessing the significance of this agreement - the effect of filtering the theoretical predictions (the geometrical limitations of the detector array) and the effect of correlations among the alpha particles emitted in the same event.

The possible effects of correlations were estimated by generating artificial events that contained no correlations and analyzing them in the same way as the real events. This was done by selecting alpha particles from different events, chosen at random, and analyzing them as if they formed a real event. This was done for both theory and experiment. We found that the experimental spectrum and the spectra from the classical dynamical model shown in Figure 3.a and 3.b were unchanged (within statistical accuracy) when alpha particles from different events were mixed. Thus, particle-particle correlations are not an important effect in this comparison. The multifragmentation events generated by the Lopez-Randrup model do contain particle-particle correlations (mutual Coulomb repulsion of alpha particles produced in the prompt decay of an isolated ^{16}O nucleus), and when those events are randomized, the folding angle spectrum becomes indistinguishable from the sequential-decay spectrum.

It is clear that filtering has a very large effect on the theoretical folding angle distribution. This is also true for the sphericity/coplanarity analysis (Fig. 4) and the spectrum of excitation energies (Fig. 5). The reason for this is that the experimental apparatus selects a particular type of collision (large impact parameters, as shown in Fig. 1) and this is a small fraction (288/14429 = 2%) of all the 4 α events. The distributions shown in Figs. 3.a and 5.a are broad because the α-α elastic scattering cross sections (particularly the random walk component) and the attractive nuclear force exerted by the target both produce alpha particles at large angles with respect to the beam. This in turn broadens the folding angle distribution and the distribution of relative kinetic energy when the angles in the laboratory system are transferred to the rest system of the four alpha particles. Introducing the experimental requirement that all alpha particles be forward of (at least) 18 degrees in the laboratory then selects those events that have a narrower distribution.

4.4 Excitation energy

The theoretical filtered excitation energy spectrum is narrower and falls off more steeply with increasing excitation energy than the experimental spectrum. Nevertheless, the overall agreement is good, particularly when one considers that this is an *ab initio* calculation of this spectrum. In the previous comparisons with theory, made in refs. 1 and 2, the experimentally observed excitation spectrum was used as input to the theoretical calculation.

5. Summary and conclusions

The predictions of the classical dynamical model of Möhring, et al., [5,6] have been compared to the experimental data of Pouliot, et al., [2] for the reaction $^{16}O+^{197}Au$ at 32.5 MeV/A. The experimental apparatus detected the forward-angle fragments (up to 18 degrees) produced by the breakup of the projectile and enabled the full kinematic reconstruction of multiple breakup events having four fragments. The dynamical model, which considers the alpha-particle degrees of freedom only, was compared to the alpha-particle channels observed in the experiment. The angular range and energy thresholds of the detector system were used to select theoretical events for comparison to the data. Overall, rather good agreement was found in the 4 α channel for the cross sections, folding angle distribution, sphericity and coplanarity distributions, and the excitation energy spectrum.

Particle-particle correlations were not found to be very important in either the experiment or the dynamical theory. The present dynamical theory, statistical models for sequential decay, and the experiment all exhibit essentially identical folding-angle and sphericity/coplanarity distributions. This makes it impossible, on the basis of the present comparisons alone, to conclude that the measured folding angle distributions *require* an interpretation in terms of sequential decay. The experimental data, however, appear to rule out the particle-particle correlations corresponding to the mutual Coulomb repulsion of alpha particles from the multifragmentation [3] of an isolated ^{16}O nucleus.

Acknowledgement

This work was supported in part by the U.S. Department of Energy under Contract No. DE-AC03-76SF00098.

References

[1] B.A. Harmon, J. Pouliot, J.A. Lopez, J. Suro, R. Knop, Y. Chan, D.E. DiGregorio, and R. G. Stokstad, Phys. Letts. **B 235** (1990) 234.

[2] J. Pouliot, Y. Chan, A Dacal, D.E. DiGregorio, B.A. Harmon, R. Knop, M.E. Ortiz, E. Plagnol, R.G. Stokstad, C. Moisan, L. Potvin, C. Rioux, and R. Roy, Phys. Letts. **B 223** (1989) 16.

J. Pouliot, Y. Chan, D.E. DiGregorio, B.A. Harmon, R. Knop, C. Moisan, R. Roy, and R.G. Stokstad, Phys. Rev. **C 43** (1991) 735.

[3] J.A. Lopez and J. Randrup, Nucl. Phys. **A 491** (1989) 477.

[4] W. Terlau, M. Bürgel, A. Budzanowski, H. Fuchs, H. Homeyer, G. Röschert, J. Uckert and R. Vogel, Z. Phys. **A 330** (1988) 303.

J. Uckert, A Budzanowski, M. Bürgel, H. Fuchs, H. Homeyer and W. Terlau, Phys. Lett. **B 206** (1988) 190

[5] K. Möhring, T. Srokowski, D.H.E. Gross, and H. Homeyer, Phys. Letts. **B 203** (1988) 210.

[6] K. Möhring, T. Srokowski, and D.H.E. Gross, Nucl. Phys **A 533** (1991) 333.

[7] J. Pouliot, Y. Chan, A. Dacal, A. Harmon, R. Knop, M.E. Ortiz, E. Plagnol, and R.G. Stokstad, Nucl . Instrum. Methods **A 270**, (1988) 69.

[8] W.D.M. Rae, A.J. Cole, A. Dacal, R. Legrain, B.G. Harvey, J. Mahoney, M.J. Murphy, R. G. Stokstad, and I. Tserruya, Phys. Lett. B 105 (1981) 417; Phys. Rev. **C 30** (1984) 158; S/B. Gazes, Y.D. Chan, E. Chavez, A. Dacal, M.E. Ortiz, K. Siwek-Wilczynska, J. Wilczynski, and R. G. Stokstad, Phys. Lett. **B 208** (1988) 194.

[9] H. Homeyer, M. Bürgel, M. Clover, Ch. Egelhaaf, H. Fuchs, A. Gamp, D. Kovar, and W. Rauch, Phys. Rev. **C 26** (1982) 1335.

[10] R. H. Siemssen, G.J. Balster, H.W. Wilshut, P.D. Bond, P.C. Crouzen, P.B. Goldhoorn, S. Han, and Z. Sujkowski, Phys. Lett. **B 161** (1985) 261.

Table 1. Breakup reaction channels

	$^{12}C+\alpha$	$^{8}Be+^{8}Be$	$^{8}Be+2\ \alpha$	$4\ \alpha$	Total
unfiltered					
events	21517	1929	19695	14429	57570
σ (mb)	411	35	345	244	1035
filtered					
events	5670	790	1519	288	8267
σ (mb)	113	15	29	5.5	163
experiment†					
σ (mb)	63	*	*	10.5	74

†The cross sections given here are for events that are recorded by the detector array and do not include events where, for example, only 3 out of 4 alpha particles were registered. The cross sections given in ref. 2 are larger than these (e.g., 25 mb instead of 10 mb for 4 α), and reflect a correction for the efficiency of the array.

*In the experiment, the cross sections for these channels are included in the 4 α cross section because of the difficulty of identifying ^{8}Be. See ref. 2 for details.

Table 2. Mean values of the sphericity and coplanarity

	Sphericity	Coplanarity	No. Events
Model			
unfiltered	0.050	0.032	14429
filtered	0.200	0.104	292
Experiment	0.191	0.101	7300

Figure Captions

1. The distribution of impact parameters leading to the 4 α channel. The requirement that all four alpha particles be emitted with polar angles less than 18 degrees selects the more peripheral collisions in the model.

2. Singles differential angular distributions for individual alpha particles observed in the 4 α and $^{12}C + \alpha$ coincidence channels. The unit solid angle $\Delta\Omega$ corresponds to a single phoswich detector. Each event in the 4 α channel contributes four counts to the distribution whereas an alpha particle in the $^{12}C + \alpha$ channel contributes one count. The filtered model and experimental angular distributions are normalized to each other for the 4 α channel as described in the text. The shape of the theoretical singles angular distribution is not changed much by the filtering.

3. The folding angle distribution in the rest frame of the 4 α system. The angle is the polar angle between alpha particles taken pair-wise. Each event contributes six counts to the spectrum. a) The theoretical distribution for all 4 α events. b) The filtered theoretical events (histogram), the experimental data (solid points), and the multifragmentation distribution from the kinematic model of ref. 3. (solid line).

4. The sphericity-coplanarity distributions for the 4 α channel. a) The experimental data. b) The dynamical model, filtered. c) The dynamical model, unfiltered. For clarity, only 175 events are shown in each of the scatter plots. The crosses indicate the average values of the sphericity and coplanarity, and were calculated using all events. The numerical values are given in Table 2.

5. The excitation energy (relative kinetic energy plus separation energy for $^{16}O \rightarrow 4\ \alpha$) in the rest frame of the 4 α system. a) Model, unfiltered. b) Model, filtered (histogram) and experimental data (solid points).

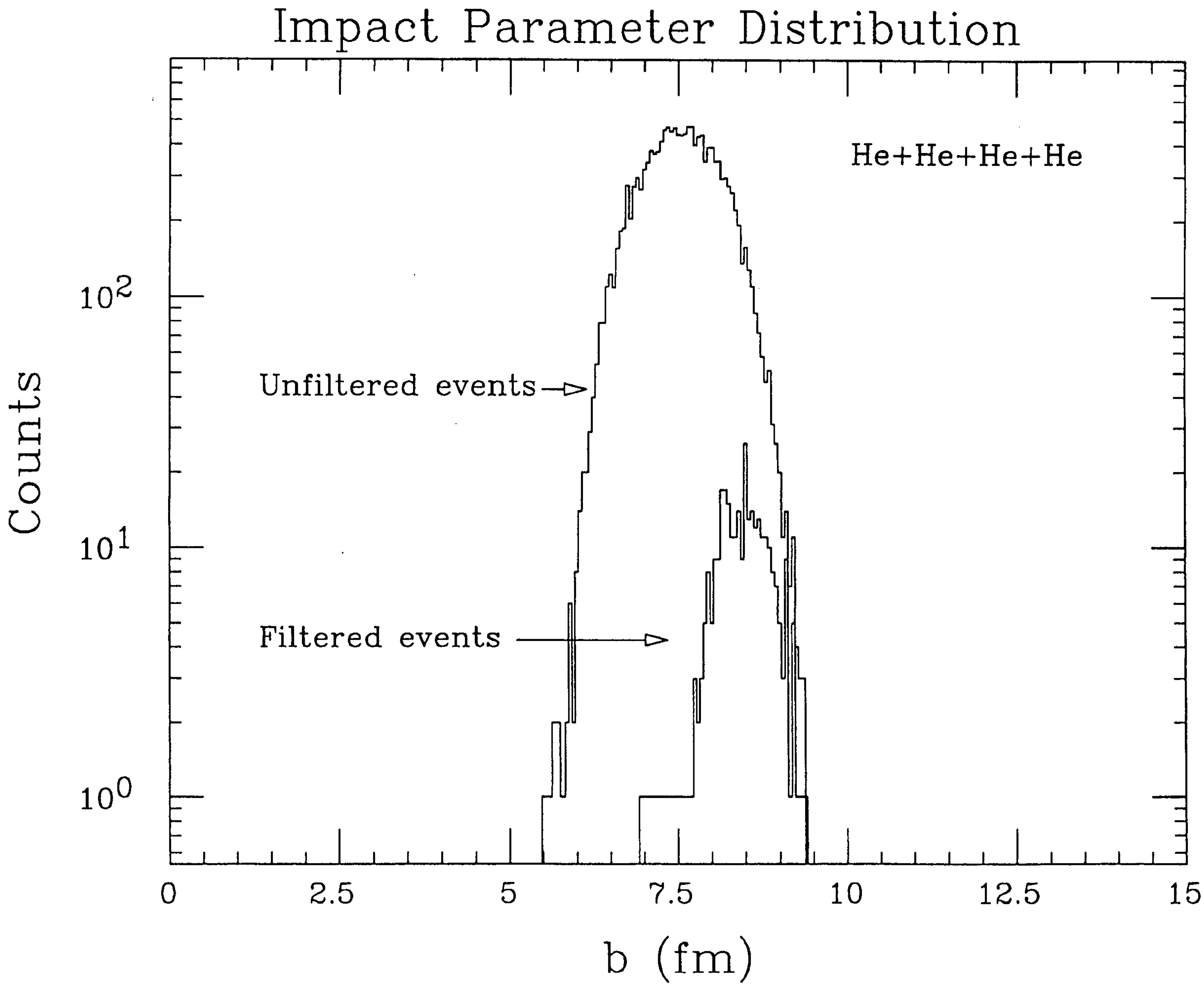
Impact Parameter Distribution
He+He+He+He
Unfiltered events
Filtered events
Counts
10^2
10^1
10^0
0
2.5
5
7.5
10
12.5
15
b (fm)

Fig. 1

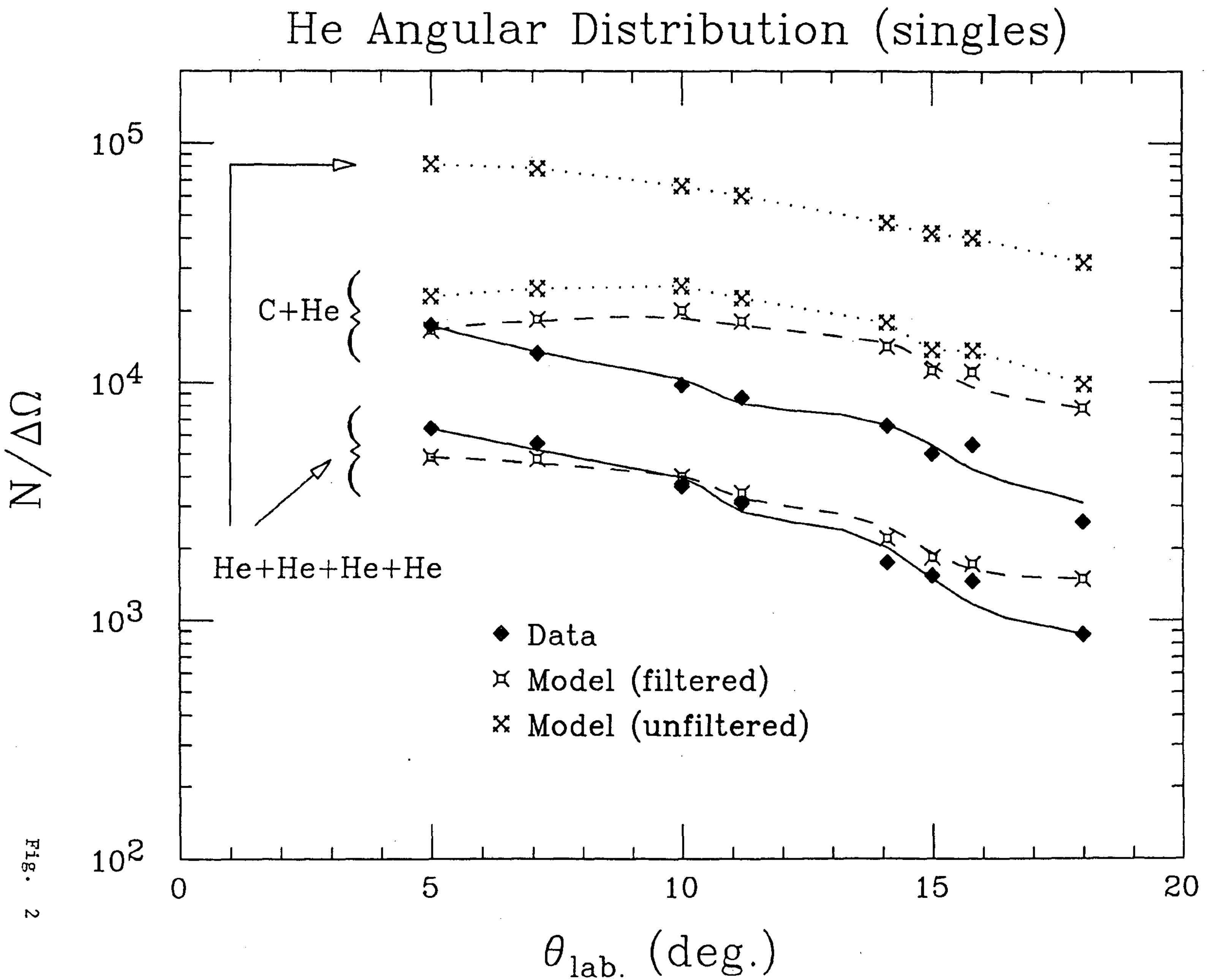
He Angular Distribution (singles)
$N/\Delta\Omega$
$\theta_{lab.}$ (deg.)
C+He
He+He+He+He
Data
Model (filtered)
Model (unfiltered)

Fig. 2

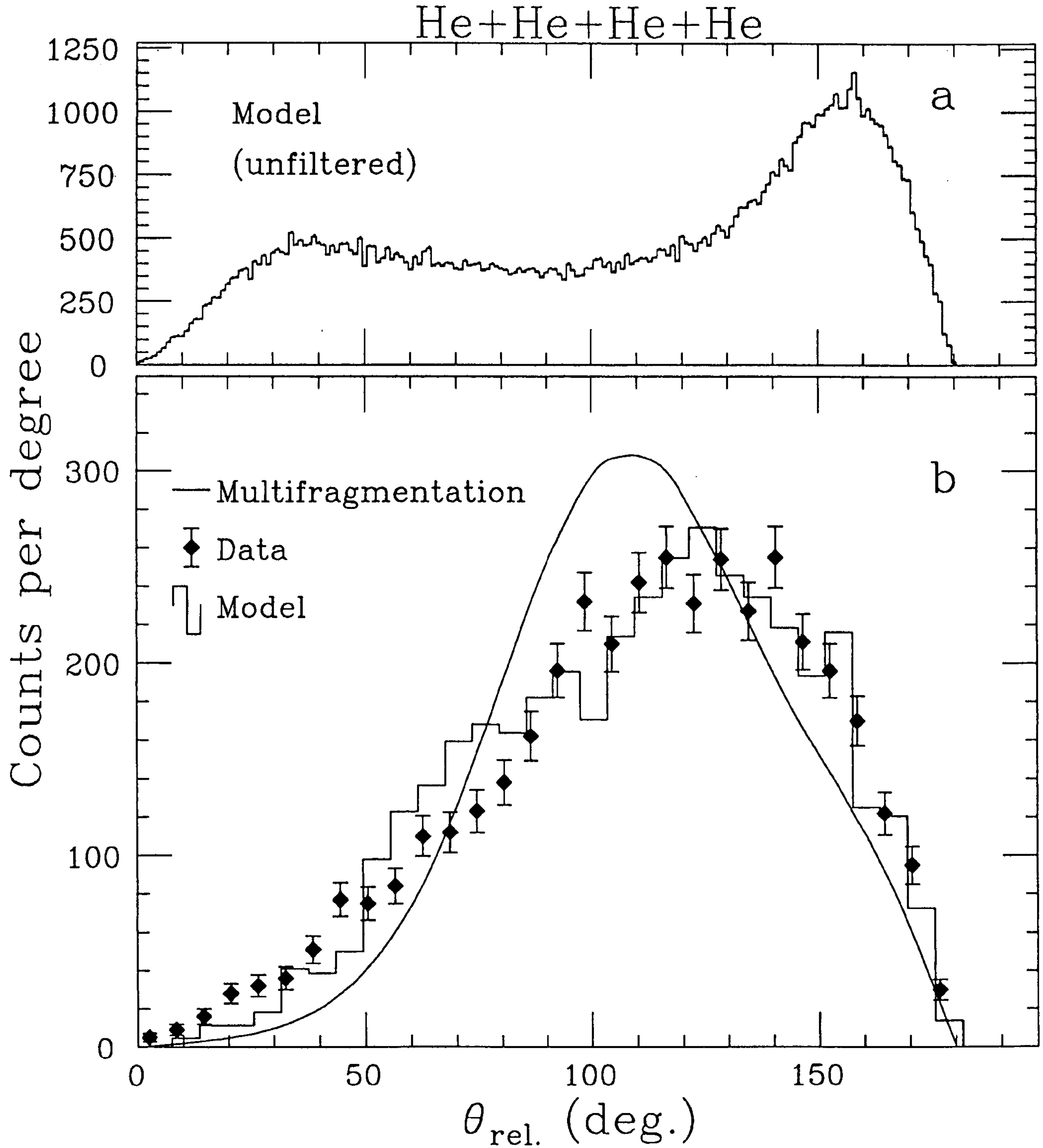
He+He+He+He
Model
(unfiltered)
a
b
Multifragmentation
Data
Model
Counts per degree
θrel. (deg.)

Fig. 3

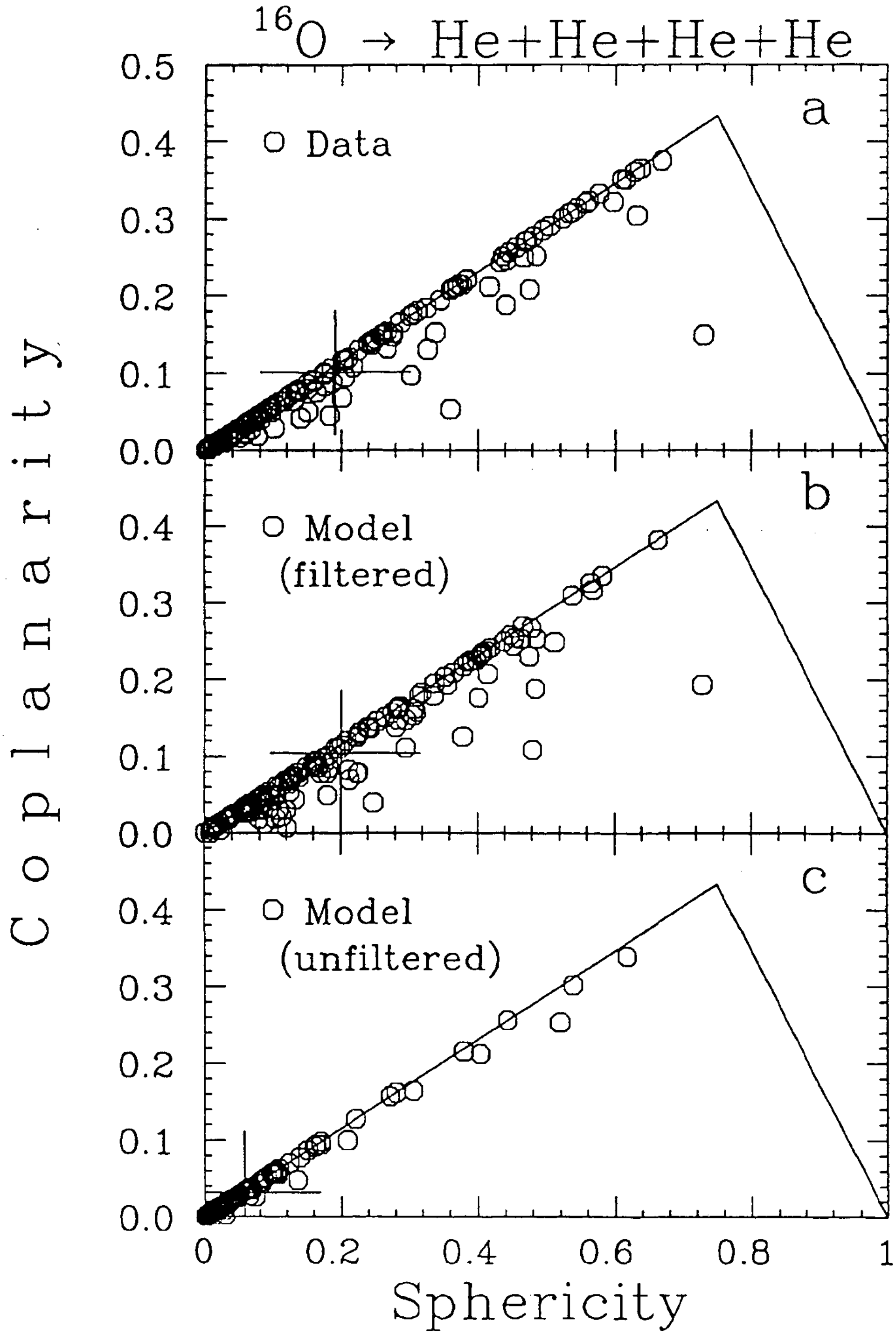
$^{16}O \rightarrow$ He+He+He+He
Coplanarity
Sphericity
a
Data
b
Model
(filtered)
c
Model
(unfiltered)
0.5
0.4
0.3
0.2
0.1
0.0
0
0.2
0.4
0.6
0.8
1

Fig. 4

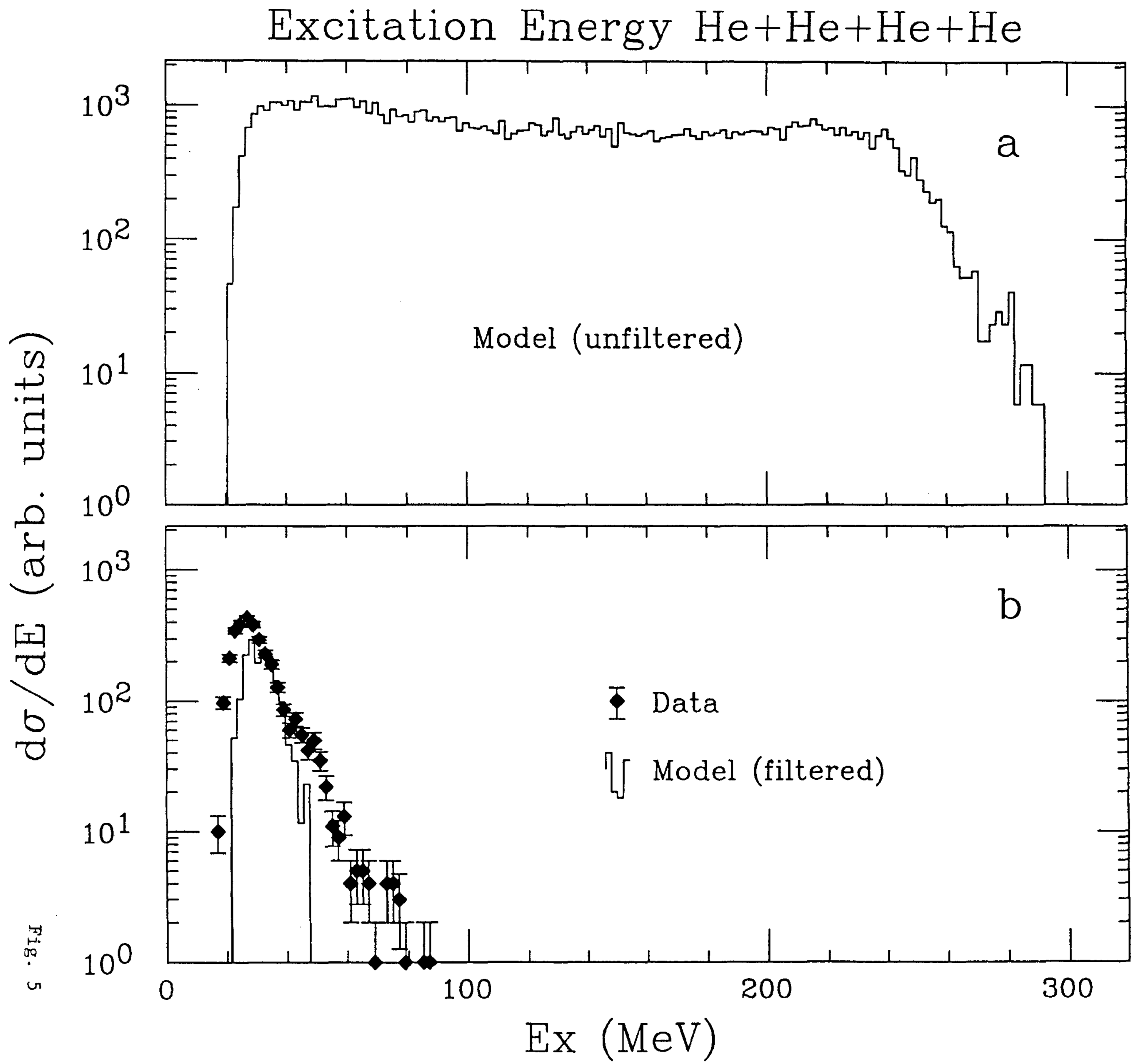
Excitation Energy He+He+He+He
a
Model (unfiltered)
b
Data
Model (filtered)
dσ/dE (arb. units)
Ex (MeV)
10^0
10^1
10^2
10^3
0
100
200
300

Fig. 5

LAWRENCE BERKELEY LABORATORY
UNIVERSITY OF CALIFORNIA
TECHNICAL INFORMATION DEPARTMENT
BERKELEY, CALIFORNIA 94720